

- 5, 3933 (1972).
- ⁴J. B. Pendry, Phys. Rev. Letters **27**, 856 (1971).
- ⁵B. I. Lundqvist, Phys. Status Solidi **32**, 273 (1969).
- ⁶A. Ignatiev, J. B. Pendry, and T. N. Rhodin, Phys. Rev. Lett. **26**, 189 (1971).
- ⁷R. E. Allen and F. W. DeWette, Phys. Rev. **179**, 873 (1969).
- ⁸R. E. Allen, F. W. DeWette, and A. Rahman, Phys. Rev. **179**, 887 (1969).
- ⁹R. E. Allen and F. W. DeWette, Phys. Rev. **188**, 1320 (1969).
- ¹⁰J. A. Venables and D. J. Ball, J. Cryst. Growth **3**, 180 (1968).
- ¹¹H. M. Kramer, G. L. Price, and J. A. Venables, in Proceedings of the Twenty-Fifth Anniversary Meeting of Emag. Institute of Physics, 1971 (unpublished).
- ¹²R. F. Steiger, J. M. Morabito, Jr., G. A. Somorjai, and R. H. Muller, Surf. Sci. **14**, 279 (1969).
- ¹³P. W. Palmberg, Surf. Sci. **25**, 598 (1970).
- ¹⁴J. M. Dickey, H. H. Farrell, and M. Strongin, Surf. Sci. **23**, 448 (1970).
- ¹⁵H. H. Farrell, M. Strongin, and J. M. Dickey, Phys. Rev. B **6**, 4703 (1972); Phys. Rev. B **6**, 4711 (1972).
- ¹⁶A. Ignatiev, A. V. Jones, and T. N. Rhodin, Surf. Sci. **30**, 573 (1972).
- ¹⁷A. Ignatiev, Ph.D. thesis (Cornell University, 1972) (unpublished).
- ¹⁸F. Ricca and A. Bellardo, Z. Phys. Chem. (Leipz.) **52**, 318 (1967).
- ¹⁹F. Ricca, R. Medana and A. Bellardo, Z. Phys. Chem. (Leipz.) **52**, 276 (1967).
- ²⁰S. Dushman, *Scientific Foundations of Vacuum Techniques* (Wiley, New York, 1962).
- ²¹F. W. Young, J. Appl. Phys. **35**, 1917 (1968).
- ²²D. L. Adams and L. H. Germer, Surf. Sci. **26**, 109 (1971).
- ²³A. Ignatiev and T. N. Rhodin, Amer. Lab. **4**(11), 8 (1972).
- ²⁴T. E. Madey and J. T. Yates, J. Vac. Sci. Technol. **8**, 525 (1971).
- ²⁵D. R. Sears and H. P. Klug, J. Chem. Phys. **37**, 3002 (1962).
- ²⁶U. Rossler, Phys. Status Solidi **42**, 345 (1970).
- ²⁷J. B. Pendry, J. Phys. C **2**, 1215 (1969).
- ²⁸J. M. Ziman, *Principles of the Theory of Solids* (Cambridge U. P., Cambridge, England, 1969).
- ²⁹L. H. Germer and A. U. MacRae, Phys. Rev. Lett. **8**, 489 (1962).
- ³⁰E. R. Jones, J. T. McKinney, and M. B. Webb, Phys. Rev. **151**, 476 (1966).
- ³¹J. T. McKinney, E. R. Jones, and M. B. Webb, Phys. Rev. **160**, 523 (1967).
- ³²R. F. Barnes, M. G. Lagally, and M. B. Webb, Phys. Rev. **171**, 627 (1968).
- ³³M. G. Lagally and M. B. Webb, in *The Structure and Chemistry of Solid Surfaces*, edited by G. A. Somorjai (Wiley, New York, 1969).
- ³⁴H. B. Lyon and G. A. Somorjai, J. Chem. Phys. **44**, 3707 (1966).
- ³⁵D. Tabor, J. M. Wilson, and T. J. Bastow, **20**, 471 (1971).
- ³⁶J. C. Quinto, B. W. Holland, and W. D. Robertson, Surf. Sci. **32**, 139 (1972).
- ³⁷S. Andersson and B. Kasemo, Solid State Commun. **8**, 1885 (1970).
- ³⁸J. M. Baker, Ph.D. thesis (Cornell University, 1970) (unpublished).
- ³⁹R. M. Goodman, Ph.D. thesis (University of California, Berkeley, 1969) (unpublished).
- ⁴⁰R. J. Reid, Surf. Sci. **29**, 623 (1972).
- ⁴¹R. M. Goodman, H. H. Farrell, and G. A. Somorjai, J. Chem. Phys. **48**, 1046 (1968).
- ⁴²D. Tabor and J. Wilson, Surf. Sci. **20**, 203 (1970).
- ⁴³F. Jona, D. W. Jepsen, and P. M. Marcus, Lecture Notes, Sixth LEED Seminar, Washington, D. C., 1972 (unpublished).
- ⁴⁴G. E. Laramore, Phys. Rev. B **6**, 1097 (1972).
- ⁴⁵B. C. Clark, R. Herman, and R. F. Wallis, Phys. Rev. **139**, A860 (1965).
- ⁴⁶F. Jona, Surf. Sci. **8**, 478 (1967).
- ⁴⁷V. G. Manzelli, V. G. Gavrilo, and E. I. Votovich, Fiz. Tverd. Tela **9**, 1483 (1967) [Sov. Phys.-Solid State **9**, 1157 (1967)].
- ⁴⁸B. W. Batterman and D. R. Chipman, Phys. Rev. **127**, 690 (1963).
- ⁴⁹R. E. Allen, J. Vac. Sci. Technol. **9**, 934 (1972).
- ⁵⁰J. M. Wilson and T. J. Bastow, Surf. Sci. **26**, 461 (1971).
- ⁵¹S. Y. Tong, T. N. Rhodin, and A. Ignatiev, following paper, Phys. Rev. B **8**, 906 (1973).

Layer-Dependent Surface Mean-Square Vibration Amplitudes by Low-Energy-Electron Diffraction*

S. Y. Tong,[†] T. N. Rhodin, and A. Ignatiev[‡]

School of Applied and Engineering Physics, Cornell University, Ithaca, New York 14850

(Received 5 January 1973)

The surface-vibration properties of solid xenon are investigated by low-energy-electron diffraction. Using no adjustable parameters, calculated layer-dependent mean-square vibration amplitudes and scattering factors of solid xenon are used to determine the surface Debye temperature of the xenon (111) face. The magnitude of inelastic electron damping as a function of incident electron energy in solid xenon is also determined. Results of the calculation are compared with experimental measurements for a range of energies from 0 to 400 eV.

I. INTRODUCTION

The study of vibrational modes at surfaces of solids is one of considerable current interest both ex-

perimentally and theoretically. Such studies are related to the understanding of the local configuration and interaction potential of ion cores at surfaces. At surfaces of solids, both the microscopic

configuration of neighboring ion cores and the short-range and long-range force laws are different from those in the bulk. Specific vibrational modes, known as surface phonons, which do not have counterparts in the bulk, have been determined theoretically for metal,¹⁻⁴ ionic crystals⁵⁻⁹ and noble-gas crystals.^{10,11} Such surface modes have vibration energies lying either in gaps of bulk phonon modes⁶⁻⁹ or are "peeled" off^{6,7} from bulk phonon energy bands. Another characteristic of surface phonons is that these modes are highly localized⁵⁻⁹ at the surface region. The vibration amplitudes of surface phonons attenuate rapidly as they go from the surface into the bulk. The existence of such localized surface vibration modes have recently been detected experimentally in ionic crystals and semiconductors by inelastic low-energy-electron diffraction (ILEED) from crystal slabs.¹² In these experiments, surface phonons are identified as discrete energy-loss peaks occurring at energies of several tens of millivolts from the incident electron energy. Theoretical studies of inelastic loss spectra from surface phonons have also been given recently.¹³⁻¹⁵

Apart from such highly localized surface vibration modes, which contribute less than 1% to the total phonon population in solids, nonattenuating phonon modes at solid surfaces (vibration modes having finite amplitudes extending into the bulk) also have distinct surface properties. Because of the absence of atoms on one side of a real surface, phonon modes at such a boundary have vibration amplitudes larger than those in the bulk. The mean-square displacement amplitude for a given layer and direction is obtained by finding the thermal average of the normal modes in that layer and direction. For a given solid, this thermal average is largest at the surface layer. Its value decreases layer by layer from the surface, reaching the bulk value at a few atomic layers from the surface. Also, because of the lack of site symmetry for atoms in surface layers, the mean-square amplitudes in different directions have different magnitudes.

To measure mean-square vibration amplitudes experimentally at solid surfaces, one can look at the temperature and energy dependences of elastically backscattered low-energy electrons (ELEED). The mean-square vibration amplitudes determine the Debye-Waller factors of vibrating atoms.¹⁶ Reference has been made¹⁷ to previous experimental studies of LEED temperature effects at surfaces of solid crystals since the initial work of MacRae and Germer.¹⁸ A variety of temperature measurements of LEED intensities for about a dozen different single-crystal metals have been referred to in the preceding paper.¹⁹⁻³⁰ In all of these measurements, a surface Debye temperature is obtained experimentally from a slope of a log₁₀

(intensity) vs temperature line drawn through the experimental points [see Eq. (7) of the preceding paper]. One should realize that this experimentally determined surface Debye temperature is an overall average of the following three contributions. First, it is the average of different orders of temperature-dependent elastic ion-core scattering vertices inside the solid. Each time an incident electron scatters off a given ion core inside the solid, the scattering cross section of that ion core is renormalized by a single Debye-Waller factor. Thus, if an electron undergoes a number of multiple scattering events before leaving the solid, its reflected intensity contains information of mixed orders of Debye-Waller factors of individual ion cores. In many metallic systems, multiple scattering events are known to be strong³¹⁻³⁵ and hence the experimental Debye-temperature contains a mixture of different orders of single-site Debye-Waller factors. Second, because the experimental Debye temperature is determined from electrons scattering from more than one layer of the solid surface, its value contains the average of mean-square vibration amplitudes of different surface layers. Third, at a given surface layer, the experimental Debye temperature takes the average of mean-square amplitudes over different directions. It is clear that any attempt to relate directly the experimental surface Debye temperature to mean-square vibration amplitudes of the surface layers must include proper provisions for the above three contributions.

Two facts are observed experimentally from measurements of surface Debye temperatures from solids¹⁷⁻³⁰: (i) In most materials the measured surface Debye temperature is lower in value than corresponding bulk values. (ii) It is observed that the measured Debye temperature is a function of incident electron energy. The measured value increases in magnitude as incident electron energy is increased. For metals, recent theoretical calculations using microscopic multiple scattering models^{36,37} have demonstrated that both of the observed behaviors can be explained qualitatively by a two-parameter model. In such calculations, a surface Debye temperature, isotropic in direction, is chosen for the outermost surface layer and a similarly isotropic bulk Debye temperature is chosen for the rest of the solid. In other words, such models properly take into account the mixing due to multiple scattering events of different orders of Debye-Waller factors but treat the average of mean-square amplitudes over layers and over different directions phenomenologically in terms of a surface and a bulk isotropic parameter.

In this paper, we report a calculation of the surface Debye temperature of crystalline xenon³⁸ and we compare our results with experimental data.^{17,39}

Thus we use a kinematic model for the elastic electron ion-core scattering in xenon. The kinematic nature of the xenon LEED spectra is discussed in the preceding paper.¹⁷ In this calculation, mean-square vibration amplitudes for each layer of the surface and for each direction in a given layer are included exactly. Furthermore, the value of electron damping in solid xenon, a highly uncertain quantity, is independently determined by comparing the energy dependence of the xenon scattering factor between theory and experiment. Thus, within the framework of the kinematic scattering model, this is a complete calculation of the surface Debye temperature in solids with no adjustable parameters. The quantitative accuracies of the calculated results depend on the validity of the kinematic model in solid xenon. However, it is significant that within the kinematic model, we can use independently determined values of layer-dependent mean-square amplitudes and scattering factors to extract from the data magnitudes of electron damping and surface Debye temperature without the use of adjustable parameters.

II. THEORETICAL METHOD

The intensity of an electron beam elastically back-scattered from a crystal slab with surfaces in the x - y plane is given by^{40, 41}

$$I(\vec{k}_f(\vec{g}_0), \vec{k}_i) = \frac{k_{f\perp}^{\text{out}}(\vec{g}_0)}{k_{i\perp}^{\text{out}}(\vec{g}_0)} \left(\frac{2m}{\hbar^2} \right) \times \left(\frac{1}{8\pi^2} \right)^2 \left| \frac{F(k_0)T(\vec{k}_f(\vec{g}_0), \vec{k}_i)}{k_{f\perp}(\vec{g}_0)} \right|^2, \quad (1)$$

where \vec{k}_i and $\vec{k}_f(\vec{g}_0)$ are, respectively, the incident and reflected momenta inside the solid. The vector \vec{g}_0 is a two-dimensional reciprocal wave vector indicating the index of the reflected beam. $T(\vec{k}_f(\vec{g}_0), \vec{k}_i)$ is the total scattering matrix of the crystal. The quantity $F(k_0)$ is a complex propagator renormalization factor in the solid.^{40, 41} Here a damping factor independent of momentum is assumed and therefore $F(k_0)$ is set equal to unity.⁴¹ Other quantities in Eq. (1) are defined by

$$k_0^2 = \frac{2m}{\hbar^2} [E - \Sigma(k_0, E)], \quad (2)$$

$$k_{f\perp}(\vec{g}_0) = -[k_0^2 - (\vec{k}_{i\parallel} + \vec{g}_0)^2]^{1/2} \vec{e}_1, \quad (3)$$

$$k_{f\perp}^{\text{out}}(\vec{g}_0) = -\text{Re} \left[\frac{2m}{\hbar^2} E - (\vec{k}_{i\parallel}^{\text{out}} + \vec{g}_0)^2 \right]^{1/2} \vec{e}_1, \quad (4)$$

$$k_{i\perp}^{\text{out}} = \left[\frac{2m}{\hbar^2} E - \vec{k}_{i\parallel}^{\text{out}2} \right]^{1/2} \vec{e}_1, \quad (5)$$

where the directions denoted by \perp and \parallel are, respectively, the perpendicular (z direction) and parallel directions (x and y directions) measured with respect to the crystal surface, \vec{e}_1 is a unit vector in the (incident) $+z$ direction, and $\vec{k}_{i\parallel}^{\text{out}}$ signifies the

parallel component of the incident beam outside of the crystal surface. Across the surface, parallel momenta are conserved:

$$\vec{k}_{i\parallel}^{\text{out}} = \vec{k}_{i\parallel}, \quad (6)$$

$$\vec{k}_{f\parallel}(\vec{g}_0) = \vec{k}_{i\parallel} + \vec{g}_0. \quad (7)$$

$\Sigma(k_0, E)$ in Eq. (2) is a complex scalar denoting electron-electron interactions in the solid. The scattering matrix $T(\vec{k}_f(\vec{g}_0), \vec{k}_i)$ of the solid is given by⁴⁰

$$T(\vec{k}_f(\vec{g}_0), \vec{k}_i) = \int e^{-i\vec{k}_f(\vec{g}_0) \cdot \vec{r}_2} T(\vec{r}_1, \vec{r}_2) e^{i\vec{k}_i \cdot \vec{r}_1} d\vec{r}_1 d\vec{r}_2 = \frac{(8\pi^2)^2}{A} \sum_n \left[e^{i[\vec{k}_i - \vec{k}_f(\vec{g}_0)] \cdot \vec{d}_n} \tau_n(\vec{k}_f(\vec{g}_0), \vec{k}_i) \right]. \quad (8)$$

For a monatomic crystal, one can divide the solid into parallel planes of unit cells containing one atom per unit cell. In Eq. (8), n is a layer index number and \vec{d}_n is a vector drawn from the origin of the surface layer to that of the n th layer. In the kinematic approximation, we set

$$\tau_n(\vec{k}_f(\vec{g}_0), \vec{k}_i) \approx t_n(\vec{k}_f(\vec{g}_0), \vec{k}_i) = e^{-W_n(\vec{k}_f(\vec{g}_0), \vec{k}_i)} t^0(\vec{k}_f(\vec{g}_0), \vec{k}_i), \quad (9)$$

where $t^0(\vec{k}_f(\vec{g}_0), \vec{k}_i)$ is the rigid-lattice individual ion-core scattering matrix and $W_n(\vec{k}_f(\vec{g}_0), \vec{k}_i, T)$ ⁴² is the quantity related to the mean-square vibration amplitudes of ion cores in the n th layer. For a monatomic crystal, the rigid-lattice scattering matrix $t^0(\vec{k}_f(\vec{g}_0), \vec{k}_i)$ is independent of layer number and can be expressed in terms of energy-dependent phase shifts as

$$t^0(\vec{k}_f(\vec{g}_0), \vec{k}_i) = - \left(\frac{\hbar^2}{2m} \right) \sum_{l=0}^{\infty} \frac{2l+1}{4\pi} P_l(\cos \theta) \frac{e^{2i\delta_l} - 1}{2i\delta_l}, \quad (10)$$

where θ is the scattering angle between \vec{k}_i and $\vec{k}_f(\vec{g}_0)$ and δ_l is the l th energy-dependent partial-wave phase shift. The quantity $W_n(\vec{k}_f(\vec{g}_0), \vec{k}_i, T)$ depends on layer index n and satisfies the relation

$$W_n(\vec{k}_f(\vec{g}_0), \vec{k}_i, T) = \frac{1}{2} \sum_{\alpha\beta} [k_f^\alpha(\vec{g}_0) - k_i^\alpha] \times \langle u_n^\alpha u_n^\beta \rangle_T [k_f^\beta(\vec{g}_0) - k_i^\beta], \quad (11)$$

where α and β refer to the x , y , and z Cartesian coordinates and u_n^α is the displacement of an ion core in the n th layer and α direction.

For crystals with noninteracting vibrational modes and fcc symmetry (e.g., xenon crystals), the mean-square amplitudes have the properties

$$\langle u_n^\alpha u_n^\beta \rangle_T = 0 \quad \text{if } \alpha \neq \beta, \quad (12)$$

$$\langle u_n^{x2} \rangle = \langle u_n^{y2} \rangle \neq \langle u_n^{z2} \rangle \quad (13)$$

for (100) and (111) surface layers,

$$\langle u_n^{x2} \rangle \neq \langle u_n^{y2} \rangle \neq \langle u_n^{z2} \rangle \quad (14)$$

for (110) surface layers, and

$$\langle u_n^{x2} \rangle = \langle u_n^{y2} \rangle = \langle u_n^{z2} \rangle \quad (15)$$

in the bulk. Using relations (12)–(15), one finds that $W_n(\vec{k}_f(\vec{g}_0), \vec{k}_i, T)$ in Eq. (11) reduces to

$$W_n(\vec{k}_f(\vec{g}_0), \vec{k}_i, T) = \frac{1}{2} g_{0x}^2 \langle u_n^{x2} \rangle + \frac{1}{2} g_{0y}^2 \langle u_n^{y2} \rangle + \frac{1}{2} [k_{i1} + k_{f1}(\vec{g}_0)]^2 \langle u_n^{z2} \rangle. \quad (16)$$

We note that $W_n(\vec{k}_1, \vec{k}_2, T)$ is nonisotropic for the surface layers. Hence the usual partial-wave expansion of $\tau_n(\vec{k}_1, \vec{k}_2)$ in terms of spherical wave functions used in multiple scattering treatments^{36,37} is not valid for the surface region. In the kinematic model, one can calculate $W_n(\vec{k}_1, \vec{k}_2, T)$ exactly without using partial-wave expansions.

For a given layer n , we define a Debye temperature $\Theta_D(n, \alpha)$ related to the mean-square amplitudes by

$$\langle u_n^{\alpha 2} \rangle = 3 \frac{\hbar^2}{M} \frac{1}{k_B \Theta_D(\alpha, n)} \left[\frac{1}{4} + \left(\frac{T}{\Theta_D(\alpha, n)} \right)^2 \right] \times \int_0^{\Theta_D(\alpha, n)/T} dx \frac{x}{e^x - 1}, \quad (17a)$$

$$\langle u_n^{\alpha 2} \rangle = 3 \frac{\hbar^2}{M} \frac{1}{k_B \Theta_D(\alpha, n)} \left[\frac{1}{4} + \frac{T}{\Theta_D(\alpha, n)} - \frac{1}{4} + \dots \right].$$

In the high-temperature limit $T \geq \Theta_D(\alpha, n)/2\pi$,

$$\langle u_n^{\alpha 2} \rangle = \frac{3 \hbar^2 T}{M k_B \Theta_D^2(\alpha, n)}. \quad (17b)$$

In Eqs. (17), M is the atomic mass of xenon and k_B is the Boltzmann's constant. We note that the surface Debye temperature $\Theta_D(n, \alpha)$ is both layer and direction dependent.

Substituting Eqs. (8) and (9) into Eq. (1), we obtain for the reflected elastic intensity

$$I(\vec{k}_f(\vec{g}_0), \vec{k}_i) \propto \left| \frac{k_{f1}^{\text{out}}(\vec{g}_0)}{k_{i1}^{\text{out}}(\vec{g}_0)} \right|^2 |t^0(\vec{k}_f(\vec{g}_0), \vec{k}_i)|^2 \times \left[\sum_n (e^{i[\vec{k}_i - \vec{k}_f(\vec{g}_0)] \cdot \vec{d}_n} e^{-W_n(\vec{k}_f(\vec{g}_0), \vec{k}_i, T)}) \right]^2, \quad (18)$$

For the specularly reflected beam of the xenon crystal (111) surface, we can write the temperature dependence of Eq. (18) explicitly as

$$I(\vec{k}(\vec{0}), \vec{k}_i) \propto C(\vec{k}_f(\vec{0}), \vec{k}_i) \left| \sum_n (e^{2in k_{i1} d_1} e^{-2k_{i1}^2 \langle u_n^{z2} \rangle}) \right|^2, \quad (19)$$

where $C(\vec{k}_f(\vec{0}), \vec{k}_i)$ is a coefficient independent of temperature T and d_1 is the perpendicular (z direction) spacing between successive layers of the solid.

Experimentally, one measures a surface Debye temperature from the slope of $\log_{10} I$ vs T plot. In other words, if $\bar{\Theta}_D$ is the experimentally measured surface Debye temperature for the (00) beam, then

one must have the relation

$$I(\vec{k}_f(\vec{0}), \vec{k}_i) \propto C(\vec{k}_f(\vec{0}), \vec{k}_i) \left| \frac{e^{-2k_{i1}^2 \langle u^{z2} \rangle}}{1 - e^{-2ik_{i1} d_1}} \right|^2, \quad (20)$$

where $\langle u^{z2} \rangle = 3\hbar^2 T / M k_B \bar{\Theta}_D^2$. Equating (19) and (20), we obtain for the surface Debye temperature

$$\left| \exp \left(- \frac{6\hbar^2 k_{i1}^2 T}{M k_B \bar{\Theta}_D^2} \right) \right| = \left| 1 - e^{(2ik_{i1} d_1) \sum_n [e^{2in k_{i1} d_1} e^{-2k_{i1}^2 \langle u_n^{z2} \rangle}] } \right|. \quad (21)$$

In order to solve Eq. (21) for $\bar{\Theta}_D$, we need to know the layer-dependent mean-square amplitude $\langle u_n^{z2} \rangle$ for each surface layer sampled by the incident electron, as well as the value of electron damping as a function of incident energy. The latter determines the magnitude of the imaginary part of k_{i1} in Eq. (21). At a fixed temperature, the energy-dependence of the experimental intensity is obtained from Eqs. (19) and (20) as

$$I^{\text{exp}}(\vec{k}_f(\vec{0}), \vec{k}_i) \propto \left| \frac{1}{k_{f1}(\vec{0})} t^0(\vec{k}_f(\vec{0}), \vec{k}_i) \right|^2 \times \left| \exp \left(- \frac{6\hbar^2 k_{i1}^2 T}{M k_B \bar{\Theta}_D^2} \right) \frac{1}{1 - e^{2ik_{i1} d_1}} \right|^2. \quad (22)$$

For a given temperature and angle of incidence, $I^{\text{exp}}(\vec{k}_f(\vec{0}), \vec{k}_i)$ is read off at each Bragg-peak energy from xenon elastic LEED intensity-energy spectra.¹⁷ The rigid-lattice scattering factor $t^0(\vec{k}_f(\vec{0}), \vec{k}_i)$ for solid xenon is determined independently using Eq. (10) and eight partial-wave phase shifts calculated from a Hartree-Fock potential.⁴³ In Figs. 1–3, we show the ion-core scattering factor

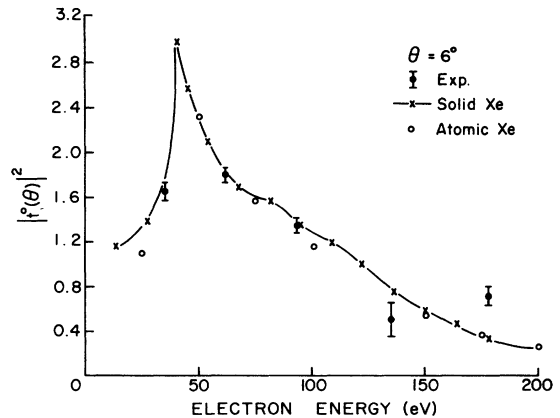


FIG. 1. Plot of ion-core scattering factor at $\theta = 6^\circ$ as a function of incident electron energy. The calculations are based on Hartree-Fock potential given in Ref. 43 (solid xenon) and atomic potential given in Ref. 44 (atomic xenon). Experimental scattering factors are extracted from data taken at $T = 61^\circ \text{K}$ (Ref. 17) using Eqs. (21) and (22), anharmonic mean-square amplitudes (Ref. 11), and electron damping values shown in Fig. 5.

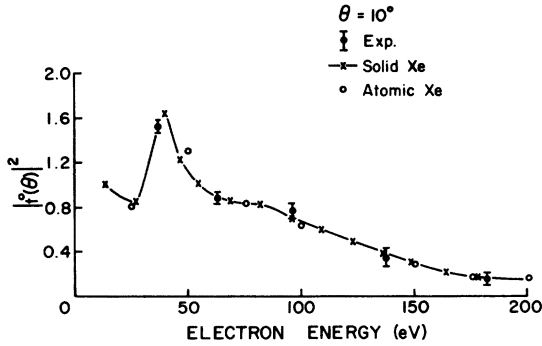


FIG. 2. Plot of ion-core scattering factor at $\theta = 10^\circ$ as a function of incident electron energy. Other details are same as in Fig. 1.

as a function of incident energy in the energy range 0–200 eV and for three different angles of incidence. For comparison, we also show the scattering factor calculated from atomic phase shifts⁴⁴ in the same energy range. The close agreement between the two theoretical calculations is not surprising, since we are looking at large backscattering angles. At such large scattering angles, the electrons mainly probe the core regions of the scattering centers. Values of $\langle u_n^{x2} \rangle$ for the Xe(111) face are taken from Allen and deWette's quasiharmonic calculation,¹⁰ from Allen, deWette, and Rahman's molecular dynamics calculation,¹¹ and from Clark, Herman, and Wallis's nearest-neighbor central-force calculation.² We show in Fig. 4 the calculated results of Allen *et al.* of $\langle u_n^{x2} \rangle$ and $\langle u_n^{z2} \rangle$ for Xe(111) surface plotted as a function of layer index n . We notice that at approximately the sixth surface layer, the mean-square amplitudes approach those in the bulk. We also note that for the Xe(111) face, $\langle u_n^{z2} \rangle$ is much larger than $\langle u_n^{x2} \rangle$ for the surface layers.

At given temperatures, using these independently determined values of $I^{\text{exp}}(\vec{k}_r(\vec{0}), \vec{k}_i)$, $t^0(\vec{k}_r(\vec{0}), \vec{k}_i)$, and

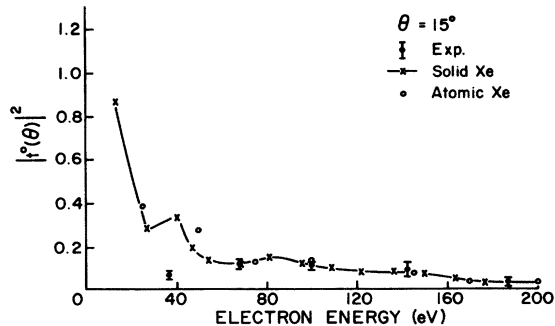


FIG. 3. Plot of ion-core scattering factor at $\theta = 15^\circ$ as a function of incident electron energy. Other details are same as in Fig. 1.

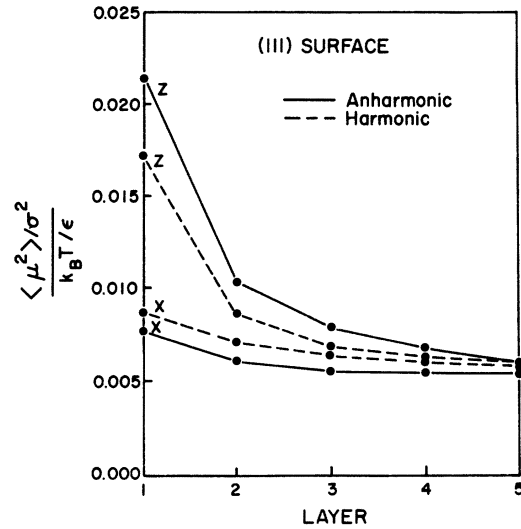


FIG. 4. Plot of surface mean-square amplitudes as a function of layer and direction of displacement. The calculations are done at half the melting temperature of xenon, $\sigma = 3.936$ and $\epsilon = 228k_B$ (other terms are self-explanatory). Data taken from Fig. 4 of Ref. 10.

$\langle u_n^{z2} \rangle$, Eqs. (21) and (22) are solved simultaneously for values of electron damping and Θ_D for each Bragg energy. The results and comparisons with experiment are discussed in Sec. III.

III. RESULTS AND DISCUSSIONS

The ratios of $\langle u_n^{x2} \rangle$ to the bulk value $\langle u_B^{x2} \rangle$ for the first five surface layers ($n = 1, 2, \dots, 5$) were taken separately from calculations of Allen *et al.*^{10,11} and Clark *et al.*² We show the ratios used for the Xe(111) face in Table I. For layers with $n \geq 6$, we assume that their mean-square amplitudes have reached the bulk amplitude $\langle u_B^{x2} \rangle$. The experimental reflected intensities $I^{\text{exp}}(\vec{k}_r(\vec{0}), \vec{k}_i)$ were taken from Xe(111) LEED data¹⁷ at 61 °K for $\theta = 6^\circ, 10^\circ$, and 15° , where θ is the angle of incidence measured from the normal to the surface.

TABLE I. Ratios of mean-square amplitudes $\langle u_n^{x2} \rangle / \langle u_B^{x2} \rangle$ for $n = 1, 2, \dots, 5$. Results are calculated from mean-square displacements from Ref. 11 (anharmonic), Ref. 10 (harmonic), and Ref. 2 (central force). For $n \geq 6$, $\langle u_n^{x2} \rangle = \langle u_B^{x2} \rangle$.

Layer n	$\langle u_n^{x2} \rangle / \langle u_B^{x2} \rangle$		Central force
	Anharmonic	Harmonic	
1	3.485	2.250	2.017
2	1.668	1.342	1.273
3	1.270	1.151	1.123
4	1.086	1.081	1.066
5	0.968	1.047	1.037
Bulk	1.000	1.000	1.000

The rigid-lattice scattering factor $t^0(\vec{k}_f, \vec{0}, \vec{k}_i)$ is calculated for the same three incident angles (see Figs. 1-3). Equations (21) and (22) are solved simultaneously for best values of electron damping and surface Debye temperature $\bar{\Theta}_D$. Values of damping thus determined, are shown in the energy range 0-200 eV in Fig. 5 (solid line). This energy range includes Bragg peaks of $n=4, 5, \dots, 8$. In Fig. 5, we show for comparison the experimental half-height widths (vertical bars) measured at $\theta = 6^\circ$ for these Bragg peaks. We also include the electron damping in solid xenon determined from mean-free-path measurements¹⁷ of iridium Auger electrons passing through the xenon crystal (crosses). Judging from Fig. 5, it seems the simple relation ΔE (peak widths at half-height) $\approx 2\Sigma_2$, where Σ_2 is the electron damping potential, holds quite well at below approximately 140 eV. Furthermore, electron damping measurements¹⁷ from Auger electrons agree excellently with damping values obtained from this work.

Above 140 eV, the experimental xenon half-widths begin to increase with energy.¹⁷ This gradual increase in the widths of peaks above 140 eV may be due to stronger multiple scattering contributions at higher energies. It could also be due to incoherent scattering of electrons from irregularities on the crystal surface.³⁷ At such higher energies, the simple relation $\Delta E \approx 2\Sigma_2$ is no longer valid. Hence, one can no longer directly determine the damping potential Σ_2 from peak widths. Microscopic calculations have used a constant value of Σ_2 for electron damping and obtained reasonable agreement with experimental LEED data.³¹⁻³⁵ We shall also use this model for Σ_2 at energies above 200 eV. Thus the electron damping value used here is determined from scattering factors up

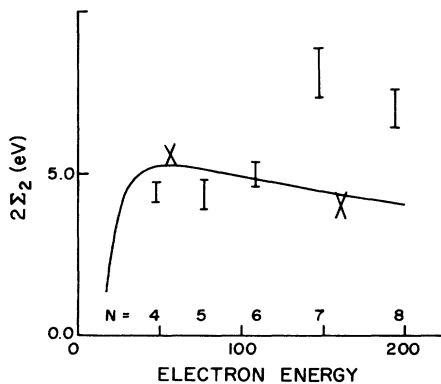


FIG. 5. Values of electron damping potential Σ_2 as a function of incident electron energy in the range 0-200 eV (solid line). Experimental peak widths at half-heights (vertical bars) taken at $\theta=6^\circ$, $T=61^\circ\text{K}$ are also shown. The crosses are values of electron damping determined from Auger electron measurements.

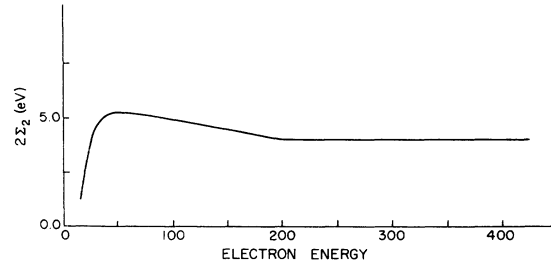


FIG. 6. Values of electron damping potential Σ_2 in the whole energy range 0-450 eV.

to 200 eV and then extrapolated at constant value to 450 eV. The damping value we used for the whole energy range 0-450 eV is shown in Fig. 6. With these values for electron damping, values of surface Debye temperature $\bar{\Theta}_D$ can be determined from Eq. (21). We show in Fig. 7 values of $\bar{\Theta}_D$ determined theoretically for $n=4, 5, \dots, 12$ and compare them with values determined experimentally from slopes of $\log_{10} I$ vs T plots. The surface Debye temperature results are plotted as a function of incident electron energy. Three sets of theoretical values are obtained using three different values of $\langle u_n^2 \rangle$ listed in Table I. The theoretical values all approach the same value of $\bar{\Theta}_{\text{Bulk}} = 43^\circ\text{K}$. This value of $\bar{\Theta}_{\text{Bulk}}$ is somewhat below the bulk Debye temperature of 56°K deduced from heat capacity measurements.⁴⁵ The difference (15.7%) may be partially explained by noting that diffraction measurements of the bulk Debye temperature and specific-heat measurements probe different regions of the phonon vibrational spectrum in a solid.¹⁷

IV. CONCLUSIONS

We have determined the surface Debye temperature for Xe(111) crystal in the energy range 0-450 eV and compared our results with experimental measurements. We have also determined the imaginary potential due to electron damping in solid xenon in the energy range 0-200 eV. The electron damping strengths thus determined compare excellently with those obtained from mean-free-path measurements¹⁷ of Auger electrons passing through solid xenon crystals in the energy range 0-200 eV. Below 140 eV, the simple relation ΔE (half-width) $\approx 2\Sigma_2$ also yields damping strengths from peak-width measurements, in good agreement with those determined here. At higher energies (above 140 eV), multiple scattering and disorder scattering seem to dominate the measured peak widths. Thus, it is no longer useful to determine damping strengths from peak-width measurements at such energies.

Above 200 eV, we have assumed a constant damping strength for Σ_2 . Values of calculated $\bar{\Theta}_D$

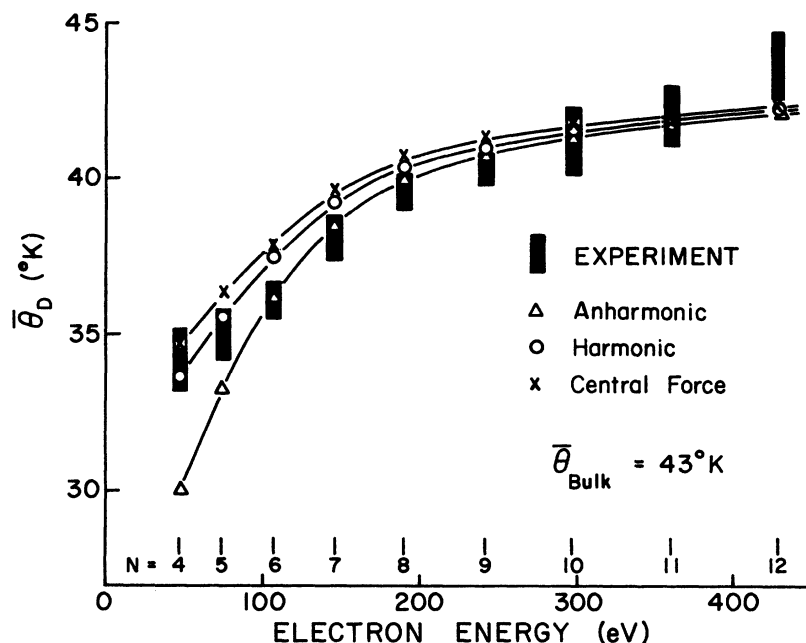


FIG. 7. Plot of theoretical and experimental surface Debye temperature $\bar{\theta}_D$ as a function of incident electron energy in the energy range 0–450 eV for Bragg peaks $n=4, 5, \dots, 12$. Note that since $\bar{\theta}_D$ is obtained from the (00) beam, only the normal (e.g., z direction) component of the mean-square vibration contributes to the analysis.

above 200 eV ($n=9, \dots, 12$, Fig. 7) are not sensitive to the magnitude of Σ_2 . The mean-square vibration amplitudes $\langle u_n^{*2} \rangle$ change most drastically for the first two surface layers (see Fig. 4). Above 200 eV, the incident electron always penetrates more than a couple of surface layers for reasonable damping strengths. A larger damping produces slightly flatter theoretical curves in Fig. 7, for $n \geq 9$.

It should again be emphasized that the extracted values of $\bar{\theta}_D$ and electron damping are dependent on the validity of the kinematic model for low-energy electron scattering in xenon crystals. It is significant, however, that within this model, we obtain reasonable agreement between theory and experiment for the extracted values of electron damping

in the energy range 0–200 eV and the trend of $\bar{\theta}_D$ as a function of energy in the range 0–450 eV.

ACKNOWLEDGMENTS

The authors are particularly grateful to R. E. Allen, F. W. deWette, and R. F. Wallis for making their mean-square vibration amplitude calculations available to us. Special thanks are expressed to J. B. Pendry for the use of his xenon phase-shift calculations. Critical discussions with B. I. Lundqvist on electron damping calculations in xenon are much appreciated. Research support to complete work on this manuscript at their respective institutions by S. Y. Tong and A. Ignatiev is also acknowledged.

*Supported principally by the National Science Foundation and partly by the Cornell Materials Science Center.

†Present address: Department of Physics, North Dakota State University, Fargo, N. D. 58102.

‡Present address: Department of Materials Science, State University of New York, Stony Brook, N. Y. 11790.

¹I. M. Lifschitz and S. I. Pekar, *Usp. Fiz. Nauk* **56**, 531 (1955).

²C. B. Clark, R. Herman, and R. F. Wallis, *Phys. Rev.* **139**, A860 (1965).

³R. F. Wallis, *Phys. Rev.* **116**, 302 (1959).

⁴A. A. Maradudin and J. Melngailis, *Phys. Rev.* **133**, A1188 (1964).

⁵R. Fuchs and K. L. Kliewer, *Phys. Rev.* **140**, A2076 (1965).

⁶S. Y. Tong and A. A. Maradudin, *Phys. Rev.* **181**, 1318 (1969).

⁷T. S. Chen, G. P. Alldredge, F. W. deWette, and R. E. Allen, *Phys. Rev. Lett.* **26**, 1543 (1971).

⁸A. A. Lucas, *J. Chem. Phys.* **48**, 3156 (1968).

⁹R. F. Wallis, D. L. Mills, and A. A. Maradudin, in *Localized Excitations in Solids*, edited by R. F. Wallis (Plenum, New

York, 1968).

¹⁰R. E. Allen and F. W. deWette, *Phys. Rev.* **179**, 873 (1969); *Phys. Rev.* **188**, 1320 (1969).

¹¹R. E. Allen, F. W. deWette, and A. Rahman, *Phys. Rev.* **179**, 887 (1969).

¹²H. Ibach, *Phys. Rev. Lett.* **24**, 1416 (1970); *Phys. Rev. Lett.* **27**, 253 (1971).

¹³V. Roundy and D. L. Mills, *Phys. Rev.* **5**, 1347 (1972).

¹⁴A. A. Lucas and M. Sunjic, *Phys. Rev. Lett.* **26**, 229 (1971).

¹⁵E. Evans and D. L. Mills, *Phys. Rev. B* **5**, 4126 (1972).

¹⁶See, for example, J. M. Ziman, *Theory of Solids* (Cambridge U. P., Cambridge, England, 1964), p. 60.

¹⁷A. Ignatiev and T. N. Rhodin, preceding paper, *Phys. Rev. B* **8**, 893 (1973).

¹⁸A. U. MacRae and L. H. Germer, *Phys. Rev. Lett.* **8**, 489 (1962).

¹⁹E. R. Jones, J. T. McKinney, and M. B. Webb, *Phys. Rev.* **151**, 476 (1966).

²⁰R. F. Barnes, M. G. Lagally, and M. B. Webb, *Phys. Rev.* **171**, 627 (1968).

²¹M. G. Lagally and M. B. Webb, in *The Structure and*

- Chemistry of Solid Surfaces*, edited by G. A. Somorjai (Wiley, New York, 1969).
- ²²H. B. Lyon and G. A. Somorjai, *J. Chem. Phys.* **44**, 3707 (1966).
- ²³D. Tabor, J. M. Wilson, and T. J. Bastow, *Surf. Sci.* **20**, 471 (1971).
- ²⁴J. C. Quinto, B. W. Holland, and W. D. Robertson, *Surf. Sci.* **32**, 139 (1972).
- ²⁵S. Andersson and B. Kasemo, *Solid State Commun.* **8**, 1885 (1970).
- ²⁶J. M. Baker, Ph.D. thesis (Cornell University, 1970) (unpublished).
- ²⁷R. M. Goodman, Ph.D. thesis (University of California, Berkeley, 1969) (unpublished).
- ²⁸R. J. Reid, *Surf. Sci.* **29**, 623 (1972).
- ²⁹R. M. Goodman, H. H. Farrell, and G. A. Somorjai, *J. Chem. Phys.* **48**, 1046 (1968).
- ³⁰D. Tabor and J. Wilson, *Surf. Sci.* **20**, 203 (1970).
- ³¹J. A. Strozier and R. O. Jones, *Phys. Rev. B* **3**, 3228 (1971).
- ³²S. Y. Tong and T. N. Rhodin, *Phys. Rev. Lett.* **26**, 711 (1971).
- ³³D. W. Jepsen, P. M. Marcus, and F. Jona, *Phys. Rev. Lett.* **26**, 1365 (1971); *Phys. Rev. B* **5**, 3933 (1972).
- ³⁴J. B. Pendry, *J. Phys. C* **4**, 2501 (1971); *J. Phys. C* **4**, 2514 (1971).
- ³⁵G. E. Laramore and C. B. Duke, *Phys. Rev. B* **5**, 267 (1972).
- ³⁶G. E. Laramore, *Phys. Rev. B* **6**, 1097 (1972).
- ³⁷F. Jona, D. W. Jepsen, and P. M. Marcus, in *Proceedings of the Sixth LEED Seminar*, Washington, D.C., 1972 (unpublished).
- ³⁸A. Ignatjevs, T. N. Rhodin, S. Y. Tong, B. I. Lundqvist, and J. B. Pendry, *Solid State Commun.* **9**, 1851 (1971).
- ³⁹A. Ignatjevs, J. B. Pendry, and T. N. Rhodin, *Phys. Rev. Lett.* **26**, 189 (1971).
- ⁴⁰S. Y. Tong, T. N. Rhodin, and R. H. Tait, *Phys. Rev. B* **8**, 421 (1973).
- ⁴¹S. Y. Tong, T. N. Rhodin, and R. H. Tait, *Phys. Rev. B* **8**, 430 (1973).
- ⁴²S. Y. Tong, T. N. Rhodin, and R. H. Tait, *Surf. Sci.* **34**, 457 (1973).
- ⁴³The symbol T in $W_n(\vec{k}_f, \vec{g}_0, \vec{k}_p, T)$ denotes the absolute temperature and is not to be confused with the total scattering matrix $T(\vec{k}_f, \vec{g}_0, \vec{k}_p)$.
- ⁴⁴J. B. Pendry (private communication).
- ⁴⁵M. Fink and A. C. Yates, *Atomic Data* **1**, 385 (1970); Teneco Report No. 88, University of Texas, 1970 (unpublished).